Acta Crystallographica Section F
Structural Biology and Crystallization Communications
ISSN 1744-3091

Crystallization and preliminary X-ray characterization of the catalytic domain of collagenase G from *Clostridium histolyticum*

Ulrich Eckhard,* Dorota Nüss, Paulina Ducka, Esther Schönauer and Hans Brandstetter

Structural Biology Group, Department of Molecular Biology, University of Salzburg, 5020 Salzburg, Austria

Correspondence e-mail: ulrich.eckhard@sbg.ac.at

Received 12 March 2008
Accepted 16 April 2008

The catalytic domain of collagenase G from *Clostridium histolyticum* has been cloned, recombinantly expressed in *Escherichia coli* and purified using affinity and size-exclusion column-chromatographic methods. Crystals of the catalytic domain were obtained from 0.12 *M* sodium citrate and 23%(*v*/*v*) PEG 3350 at 293 K. The crystals diffracted to 2.75 Å resolution using synchrotron radiation. The crystals belong to an orthorhombic space group, with unit-cell parameters $a = 57$, $b = 109$, $c = 181$ Å. This unit cell is consistent with the presence of one molecule per asymmetric unit and a solvent content of approximately 53%.

1. Introduction

Clostridium histolyticum, a Gram-positive spore-forming anaerobic bacterium that causes gas gangrene (clostridial myonecrosis) with 15–30% mortality (Burke & Opeskin, 1999; Sasaki *et al.*, 2000) was first described by Weinberg & Seguin (1916) and was given its scientific name in 1923 (Bergey *et al.*, 1923). While the histotoxicity of clostridia is primarily caused by specific toxins (Hatheway, 1990), infection is triggered by the production of various proteases including collagenases that assist in the infiltration of the host by degrading various types of collagen and gelatin (Brüggemann & Gottschalk, 2004).

Collagen is widely distributed throughout the mammalian body and is a major constituent of skin, ligaments, tendons and cartilage as well as the organic component of bones, teeth and the cornea. Furthermore, collagen is an integral component of the connective tissue that surrounds most organs. Indeed, it constitutes approximately 30% of the total protein in mammals. Consequently, any process that results in degradation or loss of integrity of this protein is likely to have significant implications for health (Harrington, 1996; Awad *et al.*, 2000). Furthermore, a diverse spectrum of biotechnological applications of bacterial collagenases exists that includes their use in meat tenderizing, as additives to laundry detergents, for wound healing, for islet-cell isolation and in the treatment of sciatica in herniated intervertebral discs or of retained placenta (Chu, 1987; Sank *et al.*, 1989; Hesse *et al.*, 1995; Fecteau *et al.*, 1998; Haffner *et al.*, 1998; Yeh *et al.*, 2002; Watanabe, 2004).

The versatility of bacterial collagenases is related to their broad substrate specificity, which has been investigated in great detail for the enzymes from *C. histolyticum*. These enzymes have been shown to display a broad substrate specificity that contrasts with the strict specificity of mammalian collagenases (Bond & van Wart, 1984; Schlage, 1988; Ravanti & Kähäri, 2000; Matsushita *et al.*, 2001; Toyoshima *et al.*, 2001; Hu *et al.*, 2002). Clostridial collagenases are large multi-modular proteins that consist of a signal peptide, a putative prodomain, a catalytic domain, one or two polycystic kidney disease-like (PKD-like) domains of unknown function and up to three collagen-binding domains (CBDs; Matsushita *et al.*, 1999; Rawlings *et al.*, 2006). With the crystal structure determination of the calcium-binding domain, a major breakthrough in the understanding of the Ca^{2+}-dependence of collagen binding and presentation has been achieved (Wilson *et al.*, 2003).

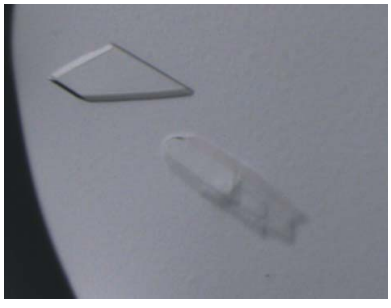

Collagenase G (ColG) from *C. histolyticum* contains 1118 amino acids and possesses a single PKD-like domain and a duplicated CBD domain in addition to the catalytic domain. Comprising approximately 670 amino acids, the latter contains the consensus motif HE*XX*H that harbours the catalytic Zn^{2+} ion. In contrast to the zinc ligation in metzincins such as MMPs, bacterial collagenases are believed to employ glutamate as a third zinc ligand (Jung *et al.*, 1999), thus belonging to the subfamily of gluzincins, albeit with a different spacing pattern to that in gluzincins of known three-dimensional structure (Kyrieleis *et al.*, 2005).

In this communication, we report the cloning, recombinant expression, crystallization and preliminary X-ray diffraction experiments of the 77 kDa catalytic domain.

2. Cloning and expression

The catalytic domain of collagenase G comprising Tyr119–Ala790 (sequence numbering according to Swiss-Prot entry Q9X721) was PCR-amplified from a cloning vector kindly provided by Roche Diagnostics GmbH using Pfu Ultra Polymerase (Stratagene). After amplification of the target gene by sense 5′-ACGTggtaccATGT-ATGATTTTGAGTATTTAAATG-3′ (*Kpn*I site in lower case) and antisense 5′-ACGTggatccTTACCCATTATCTGTTAAAACCC-3′ (*Bam*HI site in lower case) primers, the target gene was amplified by PCR using the following profile for 30 cycles after a 2 min preheat at 368 K: 30 s at 368 K, 30 s at 323 K and 2 min at 345 K. The PCR product (approximately 2000 bp) was digested with *Kpn*I and *Bam*HI and then cloned into the vector pET15b-TEV. To facilitate purification, the encoded polypeptide comprises an N-terminal hexahistidine tag separated from ColG by a TEV cleavage site. The sequence of the recombinant *col*G gene was determined by nucleotide sequencing and confirmed by comparing it with the *col*G gene of *C. histolyticum* (Matsushita *et al.*, 1999).

The recombinant plasmid was transformed into *Escherichia coli* BL21 (DE3) cells by electroporation. The induction temperature (297–310 K), the length of induction (3–6 h) and the inducer concentration (0.1–1 m*M* isopropyl *β*-D-1-thiogalactopyranoside; IPTG) were varied in the initial analysis in order to optimize the yield of soluble protein. Expression was performed in 2 l baffled flasks containing 700 ml Luria–Bertani medium containing 100 µg ml^{-1} ampicillin at 310 K with agitation at 230 rev min^{-1}; cells were grown to an OD_{600} of 1.2, induced with 0.5 m*M* IPTG and grown for 6 h at 298 K.

For the preparation of soluble protein fractions, cells from 1 l culture were harvested by centrifugation at 4500*g* for 10 min at 277 K and subsequently suspended in 25 ml ice-cold lysis buffer containing 50 m*M* Tris pH 8.0, 300 m*M* NaCl and 10 m*M* imidazole. Lysis was performed on ice by four cycles of brief sonication with 35 W pulses of 30 s duration at 3 min intervals. The lysate was cleared by centrifugation at 15 000*g* for 30 min at 277 K. All subsequent purification steps were performed at 277 K.

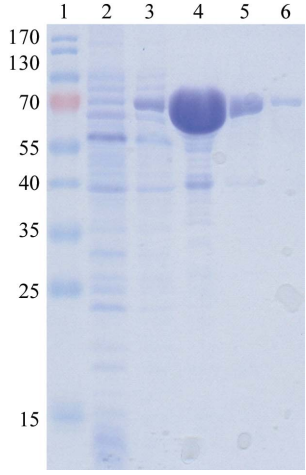

Figure 1
SDS–PAGE analysis of the catalytic domain of collagenase G during Ni–NTA purification. Proteins were analyzed on 12% SDS–PAGE and stained with Coomassie blue. Lane 1, molecular-weight markers (molecular weights are shown on the left in kDa). Lane 2, flowthrough. Lane 3, wash. Lanes 4–6, elutions.

3. Purification

Collagenase G with an N-terminal hexahistidine tag was purified using pre-equilibrated Ni–NTA resin (Qiagen). Once all unbound proteins had been washed from the column using 50 m*M* Tris pH 8.0, 300 m*M* NaCl and 40 m*M* imidazole, ColG protein was eluted from the column using 250 m*M* imidazole along with 50 m*M* Tris pH 8.0 and 300 m*M* NaCl.

The protein was concentrated to a final concentration of 10 mg ml^{-1} using a 30 kDa molecular-weight cutoff Centricon (Amicon-Ultra, Millipore). The sample was purified to ≥95% homogeneity by ÄKTA FPLC using Superdex 200 10/300 GL (Amersham Bioscience) size-exclusion column chromatography. The single peak was pooled and concentrated again to 10 mg ml^{-1}. ColG was obtained with a final yield of approximately 15 mg per litre of cell culture. The purity of the protein was judged using 12% SDS–PAGE followed by Coomassie Brilliant Blue R-250 staining and was found to be ≥95% homogeneous (Fig. 1).

4. Crystallization

Crystallization conditions were screened by the sitting-drop vapour-diffusion method using various commercial screens at 277 and 293 K. Drops were prepared by mixing 100 nl reservoir with 100 nl protein solution containing 10 mg ml^{-1} His_6-tagged protein in 25 m*M* Tris pH 7.5 and 50 m*M* NaCl and were equilibrated against reservoir solution by vapour diffusion. For pipetting, a Hydra II Plus One (Matrix Ltd) liquid-handling system was used.

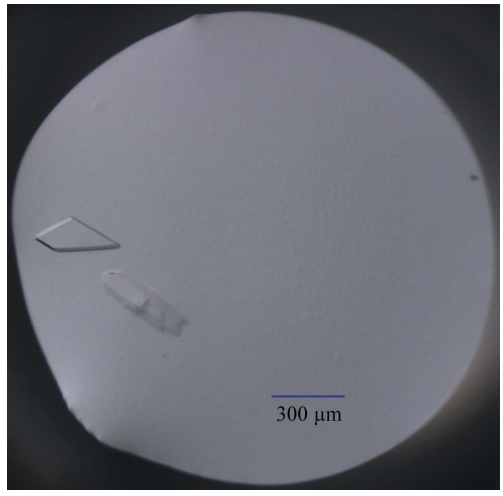

Figure 2
Crystal of the catalytic domain of collagenase G.

Table 1
Data-collection statistics.

Values in parentheses are for the highest resolution bin.

Wavelength (Å)	1.282
Space group	$P2_12_12_1$
Unit-cell parameters (Å)	a = 57.3, b = 108.7, c = 181.6
Resolution range (Å)	48–2.75
Total No. of reflections	216036 (6772)
No. of unique reflections	30180 (1049)
Completeness (%)	99.5 (97.8)
$R_{\rm merge}$†	0.127 (1.362)
$\langle I/\sigma(I)\rangle$	17.1 (2.2)
Molecules per ASU	1
Solvent content (%)	53.2

† $R_{\rm merge} = \sum_{hkl}\sum_i |I_i(hkl) - \langle I(hkl)\rangle| / \sum_{hkl}\sum_i I_i(hkl)$.

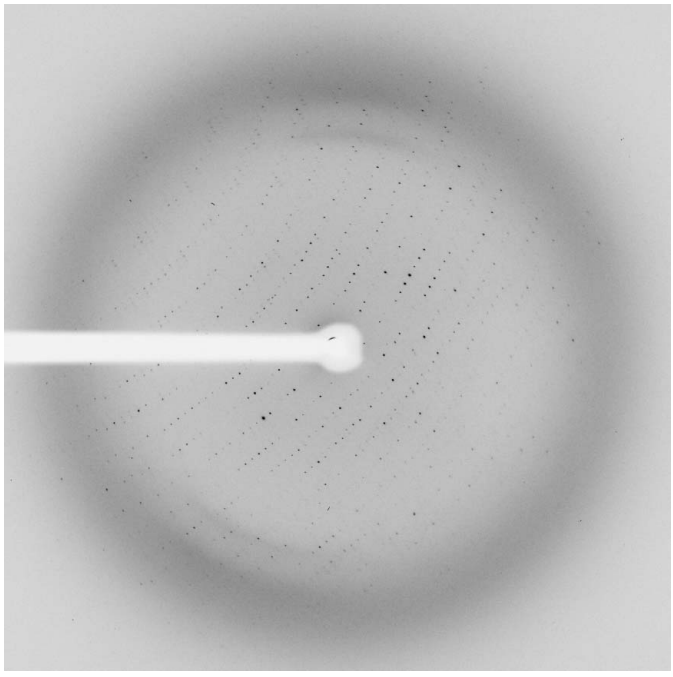

Figure 3
A representative 0.5° oscillation image obtained during data collection from a crystal of the catalytic domain of collagenase G. The frame edge is at approximately 2.4 Å resolution.

After 10 d, two small crystals were observed with reservoir conditions consisting of 0.2 *M* trisodium citrate and 20% PEG 3350 at 293 K. The size of the crystals were optimized by varying the initial crystallization conditions over the range 0.18–0.24 *M* trisodium citrate and 18–24% PEG 3350 at 293 K.

Optimization was carried out in 24-well sitting-drop format by mixing equal volumes (1.0 µl) of precipitant solution and protein solution. Crystals reached average dimensions of 0.3 × 0.1 × 0.1 mm within 10 d (Fig. 2).

5. X-ray data collection and analysis

Crystals were harvested in cryoloops; this was followed by flash-cooling in a liquid-nitrogen gas stream. Crystals were screened in-house (Bruker Microstar rotating-anode generator) with respect to diffraction limit and mosaicity and transported to beamline BM14 of the ESRF in Grenoble, France for high-resolution data collection.

The oscillation angle was 0.5° and the exposure time was 15 s per frame. A total of 360 diffraction images (Fig. 3) were recorded at a crystal-to-detector distance of 214 mm and were processed using *MOSFLM* (Leslie, 1992) and *SCALA* from the *CCP*4 suite (Collaborative Computational Project, Number 4, 1994).

A data set was collected to 2.75 Å resolution with a completeness of 99.1%. The crystals belong to the orthorhombic space group $P2_12_12_1$, with unit-cell parameters a = 57, b = 109, c = 181 Å. This unit cell is consistent with the presence of one molecule per asymmetric unit and a solvent content of approximately 53%. The statistics of data collection are listed in Table 1.

We would like to thank the EMBL Grenoble Outstation and in particular Dr Heinz Gut for providing support for measurements at the ESRF under the FP6 program and GEN-AU and Land Salzburg for their financial support.

References

Awad, M. M., Ellemor, D. M., Bryant, A. E., Matsushita, O., Boyd, R. L., Stevens, D. L., Emmins, J. J. & Rood, J. I. (2000). *Microb. Pathog.* **28**, 107–117.
Bergey, D. H., Harrison, F. C., Breed, R., Hammer, B. W. & Huntoon, F. M. (1923). Editors. *Bergey's Manual of Determinative Bacteriology*, 1st ed. Baltimore: Williams & Wilkins.
Bond, M. D. & Van Wart, H. E. (1984). *Biochemistry*, **23**, 3077–3085.
Brüggemann, H. & Gottschalk, G. (2004). *Anaerobe*, **10**, 53–68.
Burke, M. P. & Opeskin, K. (1999). *Am. J. Forensic Med. Pathol.* **20**, 158–162.
Chu, K. H. (1987). *Clin. Orthop. Relat. Res.* **215**, 99–104.
Collaborative Computational Project, Number 4 (1994). *Acta Cryst.* D**50**, 760–763.
Fecteau, K. A., Haffner, J. C. & Eiler, H. (1998). *Placenta*, **19**, 379–383.
Haffner, J. C., Fecteau, K. A., Held, J. P. & Eiler, H. (1998). *Theriogenology*, **49**, 711–716.
Harrington, D. J. (1996). *Infect. Immun.* **64**, 1885–1891.
Hatheway, C. L. (1990). *Clin. Microbiol. Rev.* **3**, 66–98.
Hesse, F., Burtscher, H., Popp, F. & Ambrosius, D. (1995). *Transplant. Proc.* **27**, 3287–3289.
Hu, Y., Webb, E., Singh, J., Morgan, B. A., Gainor, J. A., Gordon, T. D. & Siahaan, T. J. (2002). *J. Biol. Chem.* **277**, 8366–8371.
Jung, C. M., Matsushita, O., Katayama, S., Minami, J., Sakurai, J. & Okabe, A. (1999). *J. Bacteriol.* **181**, 2816–2822.
Kyrieleis, O. J., Goettig, P., Kiefersauer, R., Huber, R. & Brandstetter, H. (2005). *J. Mol. Biol.* **349**, 787–800.
Leslie, A. G. W. (1992). *Jnt CCP4/ESF–EACBM Newsl. Protein Crystallogr.* **26**.
Matsushita, O., Jung, C. M., Katayama, S., Minami, J., Takahashi, Y. & Okabe, A. (1999). *J. Bacteriol.* **181**, 923–933.
Matsushita, O., Koide, T., Kobayashi, R., Nagata, K. & Okabe, A. (2001). *J. Biol. Chem.* **276**, 8761–8770.
Ravanti, L. & Kähäri, V. M. (2000). *Int. J. Mol. Med.* **6**, 391–407.
Rawlings, N. D., Morton, F. R. & Barrett, A. J. (2006). *Nucleic Acids Res.* **34**, 270–272.
Sank, A., Chi, M., Shima, T., Reich, R. & Martin, G. R. (1989). *Surgery*, **106**, 1141–1147.
Sasaki, Y., Yamamoto, K., Kojima, A., Norimatsu, M. & Tamura, Y. (2000). *Res. Vet. Sci.* **69**, 289–294.
Schlage, W. K. (1988). *Biol. Chem. Hoppe-Seyler*, **369**, 357–363.
Toyoshima, T., Matsushita, O., Minami, J., Nishi, N., Okabe, A. & Itano, T. (2001). *Connect. Tissue Res.* **42**, 281–290.
Watanabe, K. (2004). *Appl. Microbiol. Biotechnol.* **63**, 520–526.
Weinberg, M. & Seguin, P. (1916). *C. R. Hebd. Seances Acad. Sci. Paris*, **163**, 449–451.
Wilson, J. J., Matsushita, O., Okabe, A. & Sakon, J. (2003). *EMBO J.* **22**, 1743-1752.
Yeh, C. M., Yang, M. C. & Tsai, Y. C. (2002). *J. Agric. Food Chem.* **50**, 6199–6204.